ChangSR: Super Resolution for Solder Balls on Printed Circuit Board X-Ray Image

Ting-Chi Chang (張婷淇)[1] **Chiou-Shann Fuh (傅楸善)[2]**
Zhi-Hong He (何志宏)[3] **Wei-Chen You (游惟丞)[4]**
[1,2,3,4]Department of Computer Science and Information Engineering
National Taiwan University
Taipei, Taiwan
[1]amy222024@gmail.com [2]fuh@csie.ntu.edu.tw
[3]fgghhk640@gmail.com [4]r11922197@ntu.edu.tw

Abstract

The X-ray image of Printed Circuit Board (PCB) is a crucial part in the electronics industry. Generally, the X-ray image of printed circuit board is used for rapid defect inspection to ensure the integrity of the product. The higher the resolution of the image, the subtler defects can be seen. However, if the X-ray image quality is distorted or the details disappear, it will make the defect inspection system identify errors. In recent years, many deep-learning methods have been applied to super-resolution, but most of these methods require many computer resources and much processing time.

Therefore, we mainly adopt methods such as sparse-dictionary learning and neighborhood embedding learning in traditional image processing methods to perform super-resolution processing of solder balls on the X-ray images of printed circuit boards. Thus the result of the super-resolution image is better than the result of using bicubic interpolation for super-resolution. Finally, the goal of creating high-quality super-resolution images is achieved.

Keywords: Printed circuit board, sparse-dictionary learning, neighborhood embedding learning, traditional image processing methods.

1. Introduction

Printed circuit board is indispensable basic part of various electronic products, such as computers, computer peripherals, and smart wearable devices. When the printed circuit board is defective, it will cause system failure or affect system performance. The traditional solution is direct detection by human eyes, but this method will be affected by the fatigue of the inspectors. Moreover, the definition of defects by each inspector may be different, resulting in inconsistent standards for judging defects. In order to overcome the limitations of manual inspection, it is necessary to develop an automated defect inspection system. At present, general inspectors will use the method based on computer vision to detect defects [1], automatically receive and process real-world images through optical equipment and non-contact micro-sensors. Not only can reduce the need for manual inspection, but also can be widely used in industry.

In order to make optical inspection equipment and inspector more likely to discover the welding defects of solder balls, such as holes, weld cracks, concave pits, etc., this paper mainly focuses on super-resolution of the solder balls on PCB X-ray images. Improve the quality of the X-ray image by enlarging the solder ball part in the image to ensure that there is no distortion of the solder ball part in the reconstructed high-resolution image. Super resolution is a very common research direction in the field of image processing. The related research of super-resolution is often applied in the fields of monitoring equipment, satellite images and medical imaging. Typically, a single or multiple low-resolution images are utilized to generate a high-resolution image with high quality and rich details through methods of interpolation-based, learning-based, reconstruction-based and deep-learning.

In addition, in the research of image super-resolution, it can usually be divided into two directions based on deep-learning methods and traditional image processing methods. The method based on deep-learning has the ability to process a large amount of data. It can perform complex algorithms, and automatically learn rich features in images to improve the accuracy of image super-resolution [2]. However, deep-learning models generally need to design architectures for specific problems. When the PCB boards produced by different companies need to perform super-resolution processing of solder ball images, it is generally necessary to retrain a model to adapt to their products. And it is necessary to redesign the structure of the inspection model according to the PCB board characteristics of each company. The process is very complicated and can easily take too much time. Using of traditional image processing algorithms to create super-resolution images can not only shorten the image reconstruction time, but also apply it to various types of PCB boards. There is unnecessary to adjust the algorithm for a single PCB board, and it can simultaneously satisfy the high accuracy and high speed required for t the reconstruction images of

super-resolution of solder balls.

2. Related work

Nowadays, there have been many studies on traditional image super-resolution reconstruction techniques, most of which are interpolation-based, reconstruction-based and learning-based image super-resolution methods. Therefore, the following will be mainly divided into these three parts for introduction.

2.1. The interpolation-based super-resolution method

When humans judge whether an image is of high quality or not, they often rely on the sharpness and clarity of its "edges" to make the judgment. Therefore, the edges in an image are very attractive to human vision. The main goal of edge-based interpolation is to maintain the sharpness of the edges in the image [3]. In 2001, Xin Li et al. proposed a method called New Edge-Directed Interpolation (NEDI) [4], which performs interpolation in two steps. In Step 1, interpolation is performed on two missing pixels with odd indices, and their new values are calculated by weighted averaging of their diagonal pixels. In Step 2, interpolation is performed on the pixel values above, below, to the left, and to the right, using the same principle as in Step 1, but the weights used are determined by calculating the local covariance.

Many methods have been proposed to improve NEDI, such as the Soft-decision interpolation (SAI) algorithm proposed by Zhang et al. [5], which processes a block of pixels at a time instead of a single pixel. The weights for interpolation are determined using a combination of three auto-regressive methods and Maximum a Posterior (MAP). Some researchers have also proposed improvements to the SAI method, such as the weighted least squares estimator in the RSAI method to improve the stability and accuracy of the results [6], while BSAI uses a bilateral filter to determine the weights and reduce computational complexity [7].

However, NEDI-based methods still suffer from excessive computational complexity, even higher than learning-based methods. In order to address this issue, Giachetti et al. proposed the Iterative Curvature Based Interpolation (ICBI) method [8], which also adopts the concept of NEDI 2-step interpolation. The interpolation direction is determined by computing the second order derivatives of the two directions of the pixel to be interpolated, and the energy function is used for iteration to adjust pixel values and reduce the difference with the high-resolution image.

2.2. The reconstruction-based super-resolution method

In 2015, Huang et al. aimed to reconstruct images with multiple perspectives and planes, such as buildings, and proposed the Transformed Self-Exemplars method [9]. This method can automatically search for multiple planes in the image, estimate their perspectives and affine transformations. It can generate higher quality HR images, but the disadvantage is that it requires longer calculation time.

2.3. The learning -based super-resolution method

In 2010, Yang et al. proposed a sparse coding super resolution (ScSR) method [10]. This is a single image super-resolution reconstruction algorithm based on sparse representation, which creates a dictionary by obtaining feature vectors in training samples. In fact, when super-resolution is performed, the LR image will be crop into many small patch images, and then adaptively selects the dictionary atom most suitable for the features of the current input LR patch image from the dictionary. The linear combination of these dictionary atoms is used to obtain the corresponding high-frequency details to generate HR images.

However, using ScSR for super-resolution requires more time and the image reconstruction results are not very ideal. Therefore, in 2013, Timofte et al. proposed Anchored Neighborhood Regression (ANR) [11]. This method is built on the theory of neighborhood embedding and sparse coding methods, and will find K neighbors that are closest to the features of each input patch image, and use them as its neighborhood. Then, based on each dictionary atom, the projection matrix is pre-calculated to significantly improve the execution speed during testing. The following year, Timofte et al. proposed Adjusted Anchored Neighborhood Regression (A+) [12], which performs faster and has low time complexity. This method can use fewer dictionary atoms and achieve better performance.

In 2015, Salvador et al. proposed Naive Bayes Super-Resolution Forest (NBSRF) [13]. This method has two special features. The first one is using the bimodal tree for clustering, which can calculate the set of such bimodal trees by utilizing the mapping invariance from LR to HR of patch images during the training process and providing different linear combinations of mappings. The second one is using a fast local linear search algorithm, which selects the most suitable mapping function from the tree set for each patch by adopting the local Naive Bayes formulation.

In 2017, Romano et al. proposed a Rapid and Accurate Image Super-Resolution (RAISR) [14], which focuses on image edges and can make the generated HR images sharper and clearer. This method uses a hashing algorithm to group the patch images of the training images for training, to generate a set of pre-trained filters. Then, the input LR image is first bilinearly interpolated, and the pre-trained filters are used to improve the image quality.

3. Method

In the super-resolution part of solder ball images, this paper adopts a learning-based method, A+ [12], which includes sparse-dictionary methods and neighborhood embedding methods in traditional image processing methods. And this paper makes

some adjustments on this method to perform super-resolution processing of a single solder ball image, so as to obtain a super-resolution reconstruction image that is closer to the original high-resolution solder ball image.

3.1. The A+ method

The A+ method first performs down-sampling on the input high-resolution (HR) image through an interpolation method, and divides the HR image and the low-resolution (LR) image into many HR patches and LR patches respectively. Then assuming that the LR patch and the HR patch lie on a geometric shape with local similarities, the LR patch can be described as a linear combination of its nearest neighbors, and then the corresponding HR patch can be linearly interpolated using the same coefficients, as given by Eq.(1).

$$x = C_i^* \begin{bmatrix} y \\ 1 \end{bmatrix}, with\ C_i^* = \underset{C_i}{arg\,min} \left\| y_i - C_i \begin{bmatrix} x_i \\ 1 \end{bmatrix} \right\| \quad (1)$$

Let y and x denote the LR input patch matched to cluster i and its estimated HR output patch, C_i denote the transformation matrix, and Y_i and X_i denote the training patches for cluster i.

A sparse representation of the patch space is then created by training a codebook of dictionary atoms, and then the LR and HR dictionaries are jointly trained using the sparsity constraint so that they can represent LR patches and their corresponding HR entries using a single sparse representation. When the dictionary is trained, the algorithm searches for a dense sparse representation of each input patch as a composition of dictionary atoms, as shown in Eq.(2).

$$\min_{\alpha} \|D_l \alpha - y\| + \lambda \|\alpha\| \quad (2)$$

D_l represents the LR dictionary, α is the weight matrix of the sparse selector as dictionary atom, and λ is the weight factor to balance the importance of the sparse constraint.

The characteristic of A+ is that the neighborhood of training samples may have overlapping parts. When in the neighborhood of an atom, a formula can be obtained through linear regression, and samples can be inserted from LR to HR space. Therefore, for a new LR patch, the most relevant atom in the dictionary is first found, and then the HR patch is reconstructed through the corresponding sparse representation.

3.2. The testing datasets

In order to evaluate whether the trained sparse dictionary has a certain generalization ability enough to reconstruct the super-resolution image, three different types of images are selected as testing datasets, which are solder ball dataset, Set14 dataset and Urban100 dataset. The solder ball dataset is a 3D slice generated by slicing a set of 3D reconstruction images generated by the defect inspection machine. The size of the images is 932 × 876 pixels. The Set14 dataset is a very commonly used dataset in the field of image processing. There are 14 images in total, and all of them are natural images. The maximum image size is about 768 × 512 pixels. The Urban100 dataset contains images of many different buildings, and there are 100 images in total, and the resolution of each image is not exactly the same. The maximum image size is about 1024 × 1024 pixels.

4. Experimental results

In this paper, the super-resolution experiment aims to reconstruct high-resolution images from low-resolution images that have been reduced by 4 times. Furthermore, each image has an original high-resolution image that serves as the ground truth for the experiment. This paper first uses bicubic interpolation to perform super-resolution in three testing datasets, and calculates the evaluation indicators of the super-resolution result image and the original image, such as SSIM, PSNR, etc., as the basic measurement standard for various subsequent methods and experiments. Then we directly use the A+ method to learn the sparse dictionary, and use this dictionary on three testing datasets. Figure 1 shows the super-resolution result image of one of the images in each dataset and the super-resolution image of a zoomed-in local area. Table 1 shows the numerical results of evaluation indicators such as SSIM, PSNR and MSE of super-resolution images and original high-resolution images.

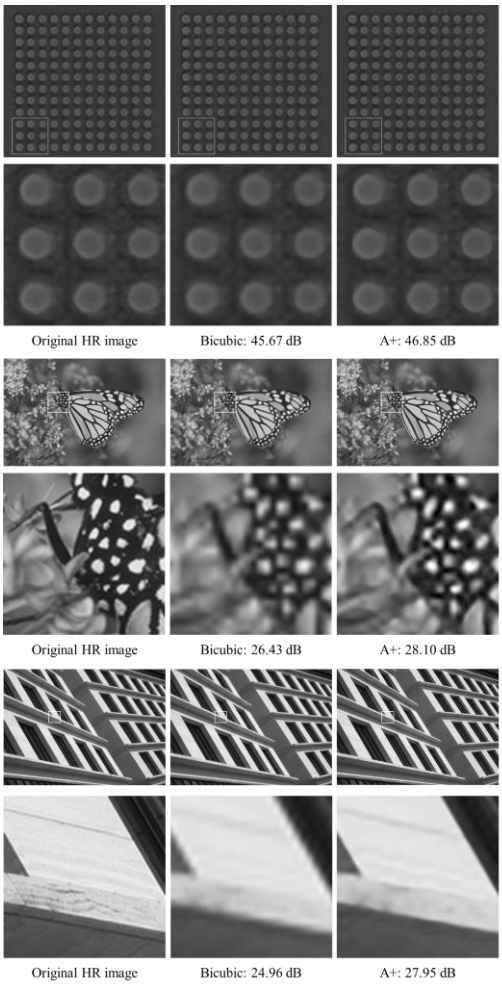

Figure 1. The super-resolution images reconstructed by bicubic and A+.

Table 1. Quantitative evaluation of bicubic and A+ methods on Solder ball, Set14 and Urban100 datasets.

	SSIM ↑	PSNR ↑	MSE ↓	TIME↓
Solder ball (A+)	**0.986484**	**47.779552**	**1.094371**	1.42
Solder ball (bicubic)	0.980399	45.166134	2.197066	**0.000995**
Set14 (A+)	**0.747422**	**25.893413**	**46.136843**	0.39
Set14 (bicubic)	0.704764	24.670395	49.841771	**0.000993**
Urban100 (A+)	**0.726183**	**23.573884**	**48.976946**	1.32
Urban100 (bicubic)	0.659958	21.909727	55.196394	**0.000974**

It can be found that the super-resolution results of the A+ method are quite good, and the super-resolution results on the solder ball image are also better than the bicubic interpolation results, but we believe that this method can still be improved. The dataset used by the A+ method contains many natural images such as flowers, plants, and human faces. Therefore, the features of the images are somewhat different from those of the solder balls. This may lead to the establishment of a learning dictionary that is not the most suitable learning dictionary for solder ball images, which limits the results of super-resolution.

Additionally, there is a paper [10] that mentions that the images of the training data set should be as diverse as possible, so we choose more circular and similar in shape to solder balls as the training dataset. There are many public image datasets available on Kaggle, from which we selected coins dataset, drugs dataset, rocks dataset, gemstones dataset. Then, in order to avoid the background of the image being too cluttered and containing too much noise, which would affect the dictionary learning, 42, 23, 21, and 102 images were selected respectively as the training datasets required for subsequent experiments.

4.1. The experiments designed for solder ball images

In the experimental part of this paper, we conducted a total of three experiments aimed at investigating the impact of training data on the super-resolution results. The first experiment is to use the coins dataset, drugs dataset, and rocks dataset, with a total of 86 images for training. The reason for this experiment is that the number of training datasets used by the original A+ is 91 images. We are concerned that not enough images in the dataset may affect the reconstruction results. Therefore, the three datasets with a relatively small number of images are integrated into a dataset and trained. The second experiment is to use only 102 images of the gemstones dataset for training. The third experiment is to integrate all 4 datasets into one dataset for training to understand whether the impact of different training data amounts on super-resolution will affect the reconstruction results. The Figure 2 shows the locally enlarged images of the super-resolution results from the first to the third experiment. Table 2 shows the average evaluation metrics results for super-resolution images and original high-resolution images from the first to third experiments.

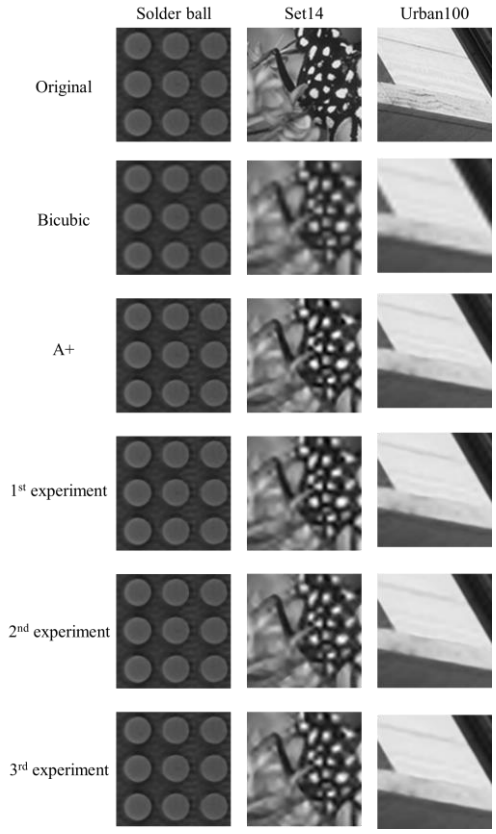

Figure 2. The enlarged images of the super-resolution results from the first to the third experiments.

Table 2. Quantitative evaluation of the solder ball, Set14, and Urban100 datasets from the first to the third experiments.

	Experiment	SSIM ↑	PSNR ↑	MSE ↓	TIME↓
Solder ball	Bicubic	0.980399	45.166134	2.197066	**0.000995**
	A+	0.985369	47.177313	1.287156	1.42
	1st experiment	0.985407	47.231209	**1.262519**	1.36
	2nd experiment	0.984914	46.969089	1.381687	1.37
	3rd experiment	**0.985521**	**47.241458**	1.265478	1.40
Set14	Bicubic	0.704764	24.670395	49.841771	**0.000993**
	A+	**0.752608**	**26.103460**	**45.232188**	0.39
	1st experiment	0.739518	25.698006	46.853918	0.37
	2nd experiment	0.744655	25.936330	45.625578	0.39
	3rd experiment	0.748910	26.033286	45.470763	0.38
Urban100	Bicubic	0.659958	21.909727	55.196394	**0.000974**
	A+	**0.722619**	**23.040200**	**50.430196**	1.32
	1st experiment	0.720552	23.025500	50.554639	1.27
	2nd experiment	0.711244	22.864230	50.753773	1.32
	3rd experiment	0.719427	23.015133	50.528270	1.33

By utilizing training images that exhibit greater diversity and more closely resemble the shapes of solder balls, it is evident that the super-resolution outcomes of solder ball images can indeed be enhanced. The lackluster results obtained from the second experiment could potentially be attributed to the homogeneity of the gemstones dataset, where most

of the images were single gemstone images, differing solely in color. Furthermore, it is noteworthy that all experimental outcomes presented in this paper have surpassed the results yielded by the widely-used bicubic interpolation technique in the field of image processing. Overall, the experiment proposed in this study helps train a sparse dictionary that is more suitable for solder ball images, and can indeed improve the super-resolution results of solder ball images. Although super-resolution processing produces higher quality images than bicubic interpolation, the processing time is several times longer, which is an area we need to improve upon.

5. Discussion

The exploration of improving the super-resolution results of solder ball images does not just stop at using diverse and similar training images, but also involves investigating the effect of using more complex images with varying amounts of training data and sizes as dictionary training images. To achieve this goal, we have extended our research to use the landscape dataset and Urban100 dataset as the training dataset to perform super-resolution reconstruction on the solder ball dataset. We designed a total of four experiments focusing on solder ball images. Through these experiments, we aimed to evaluate the effectiveness of our proposed method and further understand how to improve the super-resolution results of solder ball images.

In the fourth experiment, we selected 200 images from the landscape dataset to serve as the training dataset. In the fifth experiment, we further narrowed down the selection by taking another 100 images from the training dataset used in the fourth experiment. The sixth and seventh experiments, on the other hand, utilized the Urban100 dataset as the training dataset. It is worth noting that the image resolutions used in the sixth and seventh experiments were different, with the latter having twice the resolution of the former. Figure 3 shows the local magnification results of the 4th to 7th experiments. Table 3 presents the evaluation metrics of the results from the 4th to the 7th experiments.

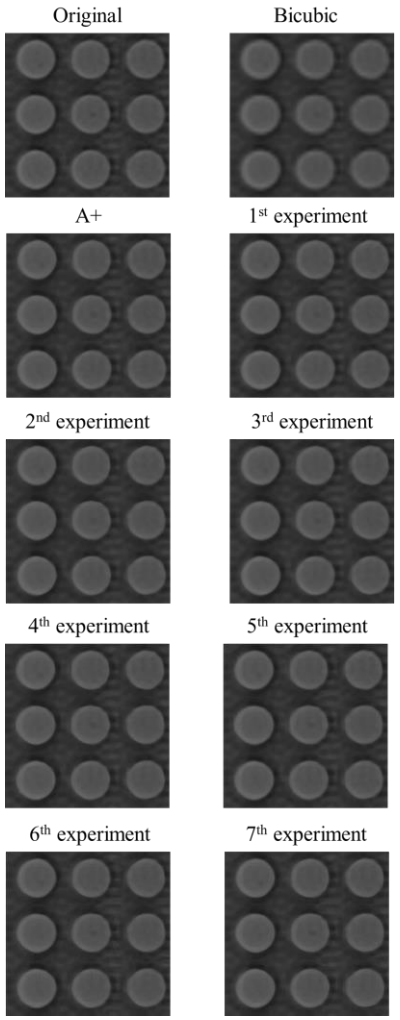

Figure 3. The enlarged images of the super-resolution results from the 4th to the 7th experiments.

Table 3. Quantitative evaluation of the solder ball dataset from the 4th to the 7th experiments.

	SSIM ↑	PSNR ↑	MSE ↓	TIME ↓
Bicubic	0.980399	45.166134	2.197066	**0.000995**
A+	0.985369	47.177313	1.287156	1.42
1st experiment	0.985407	47.231209	**1.262519**	1.36
2nd experiment	0.984914	46.969089	1.381687	1.37
3rd experiment	**0.985521**	**47.241458**	1.265478	1.40
4th experiment	0.982261	46.160476	1.685051	1.48
5th experiment	0.983089	46.507317	1.513484	1.37
6th experiment	0.979764	45.734136	1.820373	1.32
7th experiment	0.981245	45.979065	1.756360	1.40

We found that using images with complex composition, such as images of buildings, as training images for super-resolution results is not better. In terms of the results of solder ball images, the results of the original A+, the first experiment and the third experiment will be better. We consider that the possible reason is that the image textures of landscapes and buildings are too complex, and there is

no obvious subject like flowers and stone images, which affects the reconstruction results. In addition, we also found that increasing the amount of training image data does not seem to significantly improve the reconstruction results, but the higher resolution of the training images is still helpful to the reconstruction results.

6. Conclusion

This paper mainly focuses on super-resolution of the solder ball part in X-ray images of PCB to generate high-quality super-resolution images of the solder balls, making it easier to identify defective areas in the PCB. This paper evaluates the similarity between our reconstructed HR images and the original HR images using common evaluation metrics in image processing such as SSIM and PSNR. The best experiment evaluated by these metrics is the third experiment, which uses the coins, drugs, stones, and gemstones datasets for dictionary training. The average SSIM and PSNR can reach 0.9855 and 47.2415, respectively, and the execution time is about 1.4 seconds. The quality of the super-resolution images generated by our proposed experiment is better than those generated by bicubic interpolation and original A+, indicating that our proposed experiment is helpful in training a sparse dictionary more suitable for solder ball images and can indeed improve the super-resolution results by obtaining features closer to the solder balls.

Furthermore, we will try to increase the diversity of the training dataset by using different image transformation methods and look for other algorithms to find dictionary atoms. It is hoped that the execution time can be shortened while improving the super-resolution image quality, so as to achieve the purpose of fast and accurate super-resolution processing.

7. Acknowledgements

This research was supported by the Ministry of Science and Technology of Taiwan, R.O.C., under Grants MOST 111-2221-E-002-174 and MOST 109-2221-E-002-158-MY2 and by Test Research, Jorgin Technologies, III, Chernger, Jeilin Technology, Otus Imaging, D8AI, PSL, MediCapture, FIH-Foxconn, and TSMC.

8. References

[1] Z. Ren, F. Fang, N. Yan, Y. Wu, “State of the Art in Defect Detection Based on Machine Vision,” *Int. J. of Precis. Eng. and Manuf.-Green Tech*, vol. 9, pp. 661–691, 2022.

[2] W. Yang, X. Zhang, Y. Tian, W. Wang, J. -H. Xue and Q. Liao, “Deep Learning for Single Image Super-Resolution: A Brief Review,” in *IEEE Transactions on Multimedia*, vol. 21, no. 12, pp. 3106-3121, Dec. 2019.

[3] W. C. Siu and K. W. Hung, “Review of Image Interpolation and Super-Resolution,” *Proceedings of Asia Pacific Signal and Information Processing Association Annual Summit and Conference*, Hollywood, CA, pp. 1-10, 2012.

[4] X. Li and M. T. Orchard, “New Edge-Directed Interpolation,” *IEEE Transactions on Image Processing*, vol. 10, no. 10, pp. 1521-1527, 2001.

[5] X. Zhang and X. Wu, “Image Interpolation by Adaptive 2-D Autoregressive Modeling and Soft-Decision Estimation,” *IEEE Transactions on Image Processing*, vol. 17, no. 6, pp. 887-896, 2008.

[6] K. W. Hung and W. C. Siu, “Robust Soft-Decision Interpolation using Weighted Least Squares,” *IEEE Transactions on Image Processing*, vol. 21, no. 3, pp. 1061-1069, 2012.

[7] K. W. Hung and W. C. Siu, “Fast Image Interpolation using the Bilateral Filter,” *IET Image Processing*, vol. 6, no. 7, pp. 877-890, 2012.

[8] Giachetti and N. Asuni, “Real-Time Artifact-Free Image Upscaling,” *IEEE Transactions on Image Processing*, vol. 20, no. 10, pp. 2760-2768, 2011.

[9] J. -B. Huang, A. Singh and N. Ahuja, “Single image super-resolution from transformed self-exemplars,” *2015 IEEE Conference on Computer Vision and Pattern Recognition (CVPR)*, Boston, MA, USA, pp. 5197-5206, 2015.

[10] J. Yang, J. Wright, T. S. Huang and Y. Ma, “Image Super-Resolution Via Sparse Representation,” *in IEEE Transactions on Image Processing*, vol. 19, no. 11, pp. 2861-2873, 2010.

[11] R. Timofte, V. De and L. V. Gool, “Anchored Neighborhood Regression for Fast Example-Based Super-Resolution,” *2013 IEEE International Conference on Computer Vision (ICCV)*, Sydney, NSW, Australia, pp. 1920-1927, 2013.

[12] R. Timofte, V. D. Smet and L. V. Gool, “A+: Adjusted Anchored Neighborhood Regression for Fast Super-Resolution,” *Computer Vision -- ACCV 2014*, Singapore, vol. 9006, pp 111–126, 2014.

[13] J. Salvador and E. Pérez-Pellitero, “Naive Bayes Super-Resolution Forest,” *2015 IEEE International Conference on Computer Vision (ICCV)*, Santiago, Chile, pp. 325-333, 2015.

[14] Y. Romano, J. Isidoro and P. Milanfar, “RAISR: Rapid and Accurate Image Super Resolution,” *in IEEE Transactions on Computational Imaging*, vol. 3, no. 1, pp. 110-125, 2017.